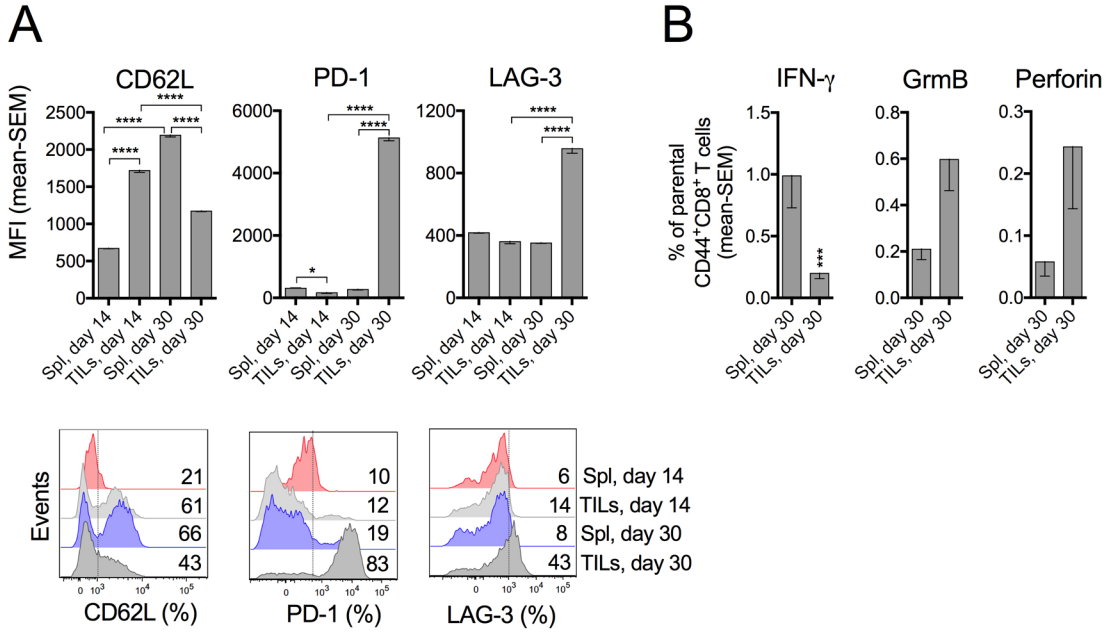

Figure S1, related to Figure 1. (A) MFI and representative flow plots of CD62L, PD-1 and LAG-3 on transferred OT-1 $CD8^+$ T cells isolated from Spl and tumors of mice bearing day 14 or 30 $B16_{OVA}$ tumors. (B) Functions of OT-1 $CD8^+$ T cells producing IFN-γ, GrmB and perforin from Spl and tumors of mice bearing day 30 $B16_{OVA}$ tumors. (A-B) n=5 mice/group. Data are shown as mean - SEM and represent at least two independent experiments.

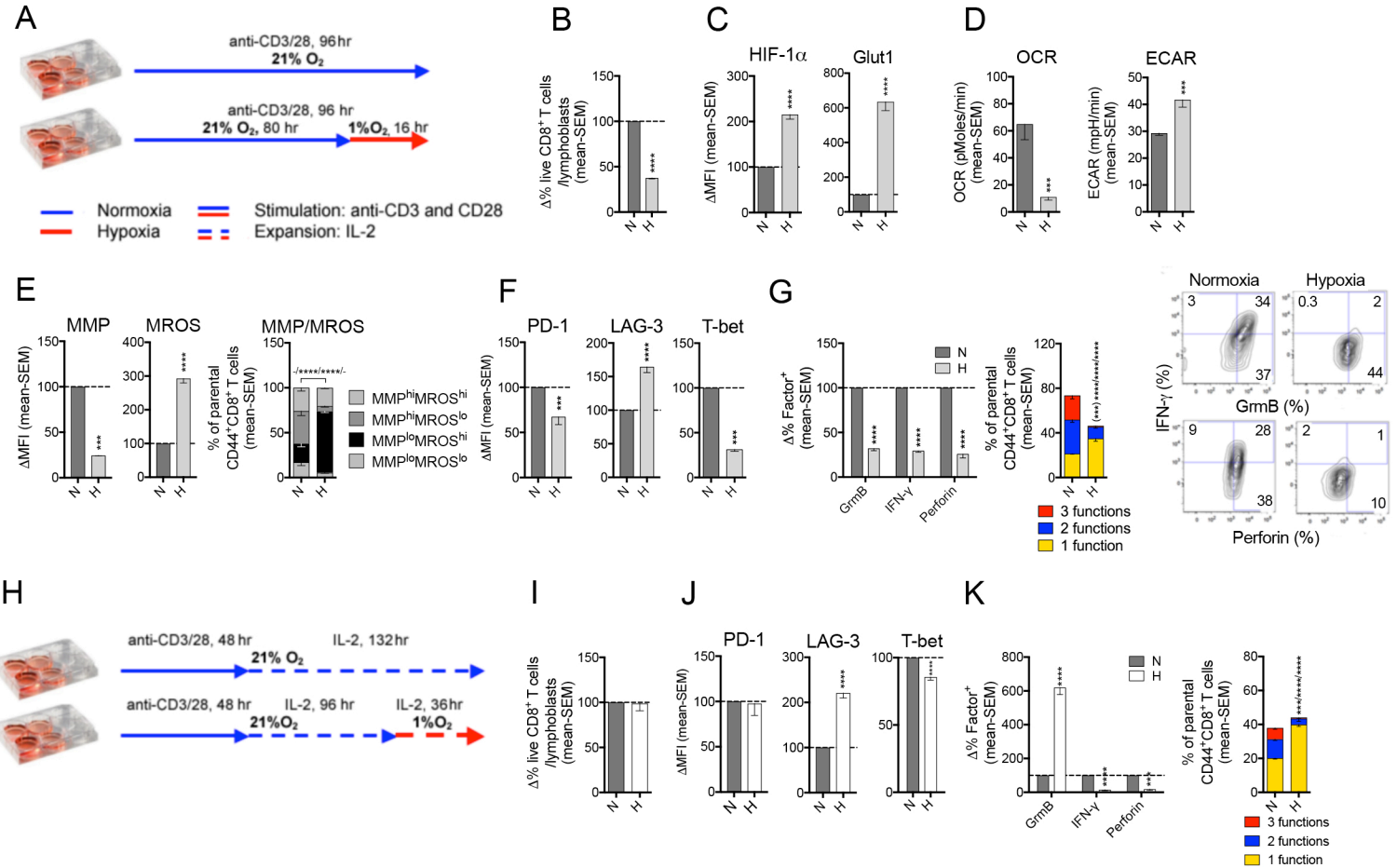

Figure S2, related to Figure 3. Hypoxia affects CD8$^+$ T cell metabolism, differentiation and functions *in vitro*. (A-G) Effect of hypoxia on activated CD8$^+$ T cells. Enriched CD8$^+$ T cells were stimulated continuously for 96 hr and cultured under 1% O_2 for the last 16 hr. (A) Experimental design. For A and H: Blue indicates Normoxia (N); red indicates Hypoxia (H); Solid line: Ab-mediated stimulation; Dashed line: culture in IL-2 without stimulation. (B) Normalized % live CD8$^+$ T cells forming lymphoblasts by day 4 of culture comparing H to N treated samples. (C) Normalized MFI for HIF-1α and Glut1 in/on CD8$^+$ T cells cultured under N or H. (D) Basal OCR and ECAR of day 4 activated CD8$^+$ T cells cultured under N or H. (E) Left: Normalized MFI for MMP and MROS stains. Right: Quadrants gating for MMP over MROS stains. $^-$ or * from left to right indicates differences between populations of MMP^{hi}MROS^{lo} cells, MMP^{hi}MROS^{hi} cells, MMP^{lo}MROS^{hi} cells and MMP^{lo}MROS^{lo} cells respectively. (F) Normalized MFI of PD-1, LAG-3 and T-bet. (G) Left: Normalized production of individual factors by cells cultured under H vs. N. Right: Functions of CD8$^+$ T cells shown as % CD44$^+$CD8$^+$ T cells producing 3, 2 or 1 of the 3 tested functions and representative flow plots. (B-G) n=4-5/condition, representative of 3-5 assays. Spleens from 20-30 mice were pooled for each assay. (H-K) Effect of hypoxia on relatively resting CD8$^+$ T cells. T cells were stimulated for 48 hr and then switched to IL-2-containing medium without additional stimulation. The effect of hypoxia was assessed by subjecting cells cultured in IL-2 to 1 % O_2 for the last 36 hr. (H) Experimental design. (I) Normalized % live IL-2-maintained CD8$^+$ T cells forming lymphoblasts comparing N to H treated samples. (J) Normalized expression of PD-1, LAG-3 and T-bet on/in cells subjected to N vs. H. (K) Left: Normalized production of individual factors by CD8$^+$ T cells comparing N vs. H treated samples. Right: % cells positive for 3, 2 or 1 of the 3 tested functions. (I,J) n=6/condition. (K) n=5 /condition. (I-K) Data represent 3 experiments and show as mean - SEM.

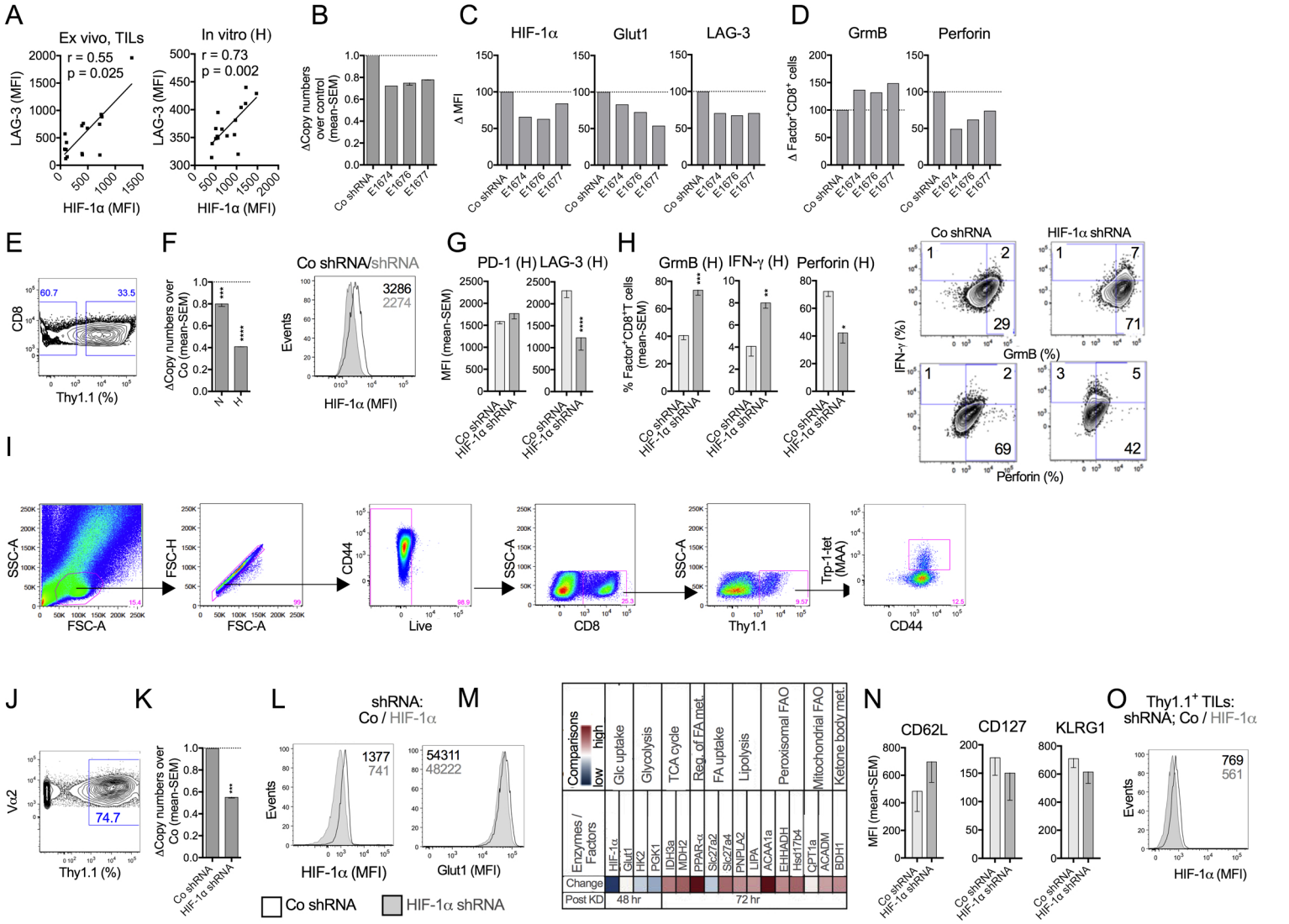

Figure S3, related to Figure 3. Effects of HIF-1α on anti-CD3/CD28-activated CD8$^+$ T cells or peptide-activated OT-1 CD8$^+$ T cells. (A) Pearson correlation between MFI values of HIF-1α and LAG-3 in/on vaccine-induced TILs or *in vitro* activated CD8$^+$ T cells that had been subjected to H. Correlation coefficient r and p values are shown. Each dot represents one sample. (B-H) Effects of HIF-1α KD on CD3/CD28-activated CD8$^+$ T cells *in vitro*. (B) Normalized reduction of HIF-1α transcripts in cells transduced with different HIF-1α shRNA lentivectors (E1674, E1676 and E1677) vs. those transduced with scrambled shRNA lentivector. (C) Normalized MFIs for HIF-1α, Glut1 and LAG-3 expression in/on cells of different groups. (D) Normalized % of cells from different groups producing cytolytic proteins upon *in vitro* stimulation. (B-D) Samples of each group were splenocytes pooled from 3 mice. Data show mean values and represent 2 experiments. (E) Levels of Thy1.1 expression upon transduction of CD8$^+$ T cells with the Thy1.1 expressing lentivector. (F) Left: Levels of HIF-1α KD under N and H determined by testing sorted Thy1.1$^+$CD8$^+$ T cells for HIF-1α transcripts (n=4/group, representative of 3 experiments). Data show normalized copy numbers in cells transduced with HIF-1α shRNA lentivector E1676 over those transduced with scrambled lentivector. Right: Representative histogram for HIF-1α expression in activated CD8$^+$ T cells transduced with control (open) or E1676 (grey) and cultured under H (represents 2 assays). (G) MFI of PD-1 and LAG-3 on activated CD8$^+$ T cells transduced with control or E1676 lentivector and cultured under H (n=6). (H) Left: % CD44$^+$CD8$^+$ T cells producing individual factors after short-term H (n=5). Right: Representative flow plots show quadrant gating for IFN-γ over GrmB or perforin. (I) Gating strategy for analyses of lentivector-transduced MAA-specific TILs in the vaccine model. (J-O) OT-1 transfer model. (J) Levels of Thy1.1 expression upon transduction of OT-1 CD8$^+$ T cells with the Thy1.1 expressing HIF-1α shRNA lentivectors. (K) Level of HIF-1α transcripts in sorted lentivector-transduced OT-1 Thy1.1$^+$CD8$^+$ T cells (n=3). (L) Expression of Glut1 and HIF-1α by lentivector-transduced OT-1 CD8$^+$ T cells; grey: HIF-1α shRNAs, open: scrambled shRNA. Numbers show MFI. (M) Heatmap: Effects of HIF-1α KD on gene expression at 48 and 72 hr after lentivector transduction. Cells in each group were sorted based on Thy1.1 expression and levels of transcripts were compared (n=3/group). (N) Expression of CD62L, CD127 and KLRG1 on transduced OT-1 TILs isolated from recipient tumors 14 days after cell transfer. (O) Flow plot shows level of HIF-1α KD in transduced OT-1 CD8$^+$ TILs recovered from recipient tumors. (N-O) n=5-8 mice/group. For each model data are representative of at least 2 experiments. Bar graphs show mean - SEM.

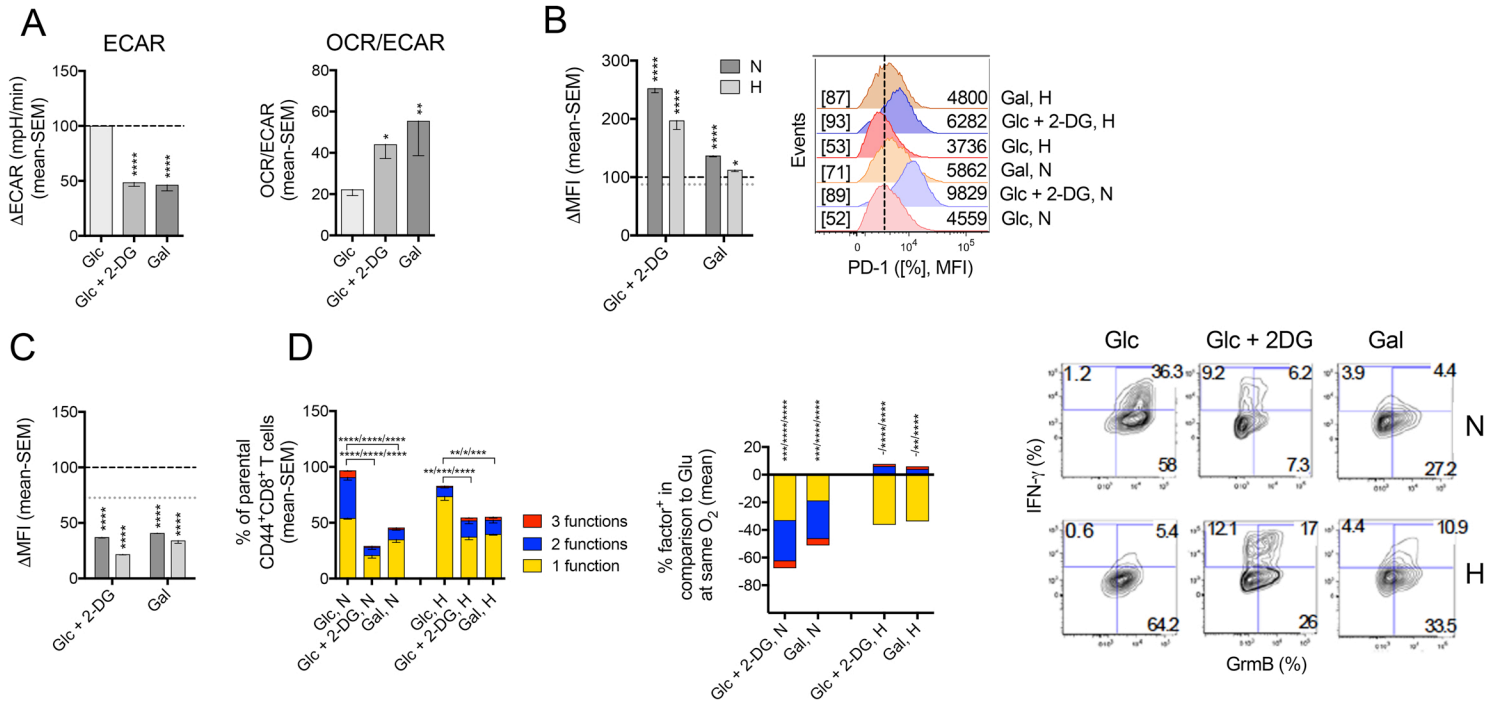

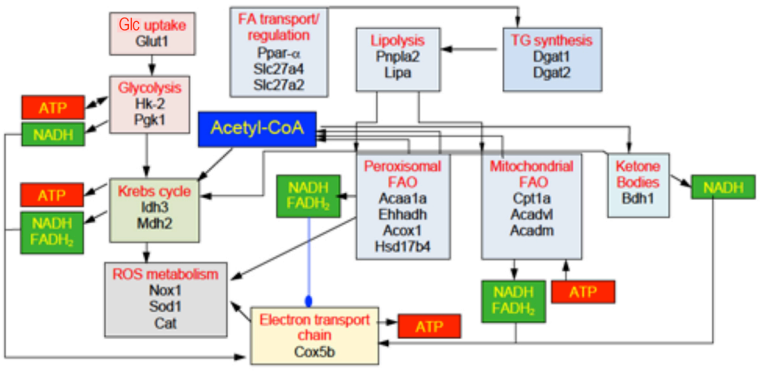

Function	Name	Abbreviation
Gucose uptake	glucose transporter 1	Glut1
Glycolysis	hexokinase 2	Hk-2
	phosphoglycerate kinase	Pgk1
TCA cycle	isocitrate dehydrogenase subunit alpha	Idh3a
	monodehydroascorbate reductase 2	Mdh2
Regulation of FA metabolism	peroxisome proliferator-activated receptor alpha	Ppar-α
FA transport	solute carrier family 27a4	Slc27a4
	solute carrier family 27a2	Slc27a2
Triglyceride (TG) synthesis	diacylglycerol O-acyltransferase 1	Dgat1
	diacylglycerol O-acyltransferase 2	Dgat2
Triglyceride (TG) catabolism	lipase A	Lipa
	patatin-like phospholipase domain containing 2	Pnpla2
Peroxisomal FAO	acetyl-CoA acyltransferase 1	Acaa1a
	CoA dehydrogenase	Ehhadh
	acyl-CoA oxidase 1	Acox1
	hydroxysteroid (17-beta) dehydrogenase 4	Hsd17b4
Mitochondrial FAO	carnitine palmitoyltransferase 1a	Cpt1a
	acyl-CoA dehydrogenase, very long chain	Acadvl
	acyl-CoA dehydrogenase, C-4 to C-12 straight chain	Acadm
Metabolism of ketone bodies	3-hydroxybutyrate dehydrogenase 1	Bdh1
ROS metabolism	NADPH oxidase 1	Nox1
	superoxide dismutase 1	Sod1
	catalase	Cat
Electron transport chain	cytochrome c oxidase subunit Vb	Cox5b

Figure S4, related to Figure 4. Effects of Glc limitation on metabolism, differentiation and effector functions of CD8$^+$ T cells activated *in vitro* under normoxia or short-term hypoxia. Where indicated (Δ in Y-axis title) values are normalized to those obtained with cells from Glc-cultures kept at N, which are set at 100 (dot black lines). The stippled light grey lines show results for cells cultured in Glc and subjected to H normalized to results for cells cultured in Glc under N. (A) Normalized basal ECAR and OCR to ECAR ratios at baseline for CD8$^+$ T cells stimulated in regular Glc-medium, Glc with 2-DG or Gal-medium for 4 days; n=4, pooled from 20 mice/experiment and representative of 3 experiments. (B) Normalized MFI and representative histograms for PD-1 expression on CD8$^+$ T cells activated under N or H. (C) Normalized MFI for T-bet. (B-C) n=4-5/condition, representative of at least 5 assays. (D) Left: % cells producing 3, 2 or 1 of the 3 tested functions over all CD44$^+$CD8$^+$ T cells cultured under different conditions. Middle: Same data as left illustrating differences in % cells producing 3, 2 or 1 functions in Glc+2-DG- or Gal-medium compared to cells in Glc-medium with the corresponding O_2 supply. Statistics on each bar indicates difference in % cells producing 3, 2 or 1 functions (bottom to top). Right: representative flow plots show IFN-γ and GrmB levels (n=4-5/condition, representative of at least 3 assays). (E) Cartoon shows roles of the different molecules that were analyzed at the transcriptional level. (F) Table summarizes the functions, names and abbreviations of each factor analyzed. (A-D) Data show mean - SEM.

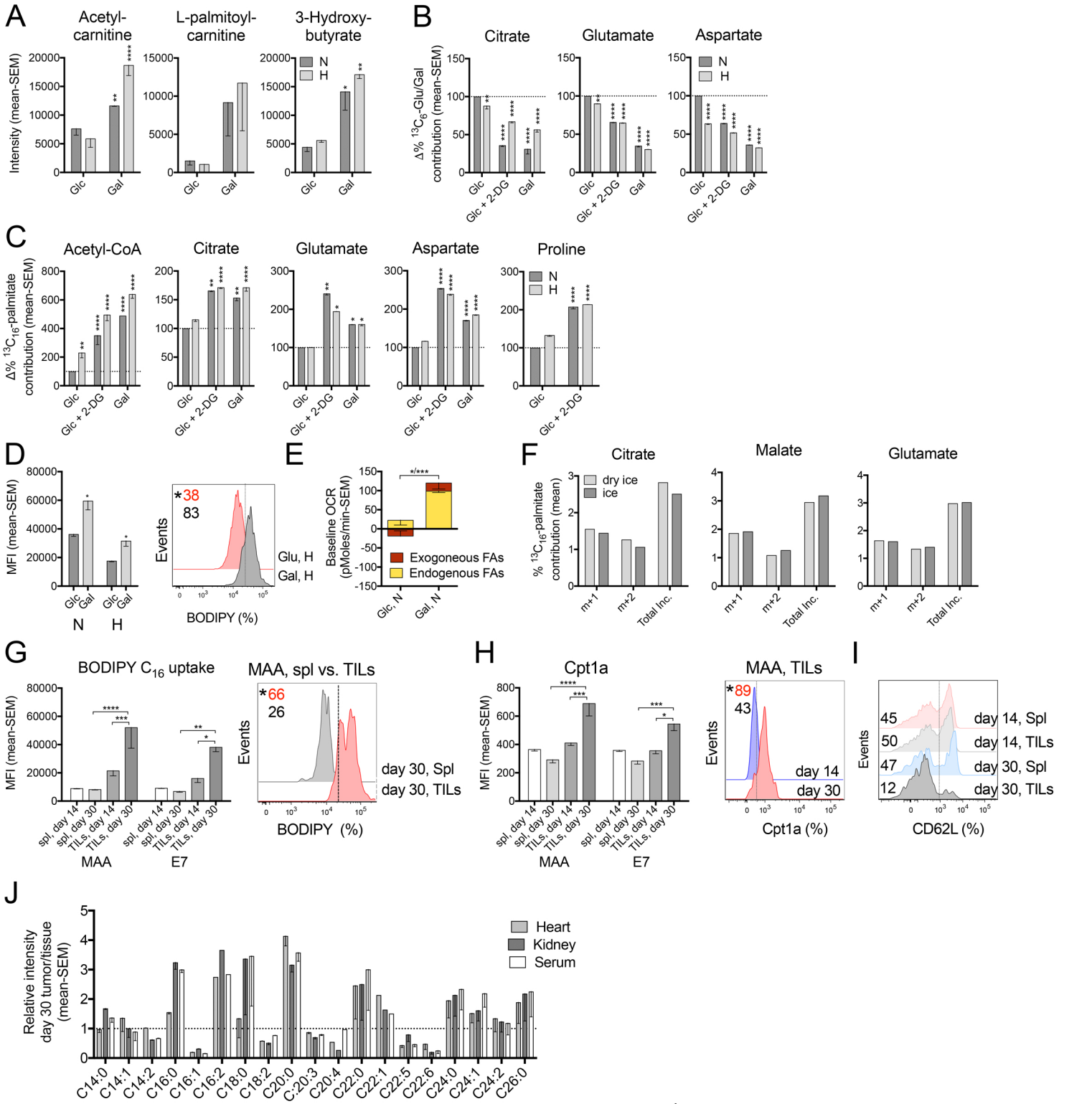

Figure S5, related to Figure 4. Effects of Glc and O_2 limitation on CD8$^+$ T cell metabolism. (A) Intensity of FA catabolism-related metabolites in CD8$^+$ T cells stimulated for 4 days *in vitro* under different conditions. N: dark grey; H: light grey. (B) Normalized contribution of $^{13}C_6$-Glc/Gal- or (C) $^{13}C_{16}$-palmitate-derived carbons to metabolites in cells cultured under different conditions compared to those cultured in Glc-medium under N (set at 100). (A-C) Enriched CD8$^+$ T cells were pooled from 20-30 mice for each experiment; data are representative of 2 experiments. * Shows significant differences compared to cells cultured in Glc-medium under N. (D) Uptake of BODITY C_{16} FA by cells cultured in Glc- or Gal- medium under N or H. Histograms show FA uptake in representative samples subjected to H (n=5, reflecting two experiments). (E) Basal OCR due to consumption of exogenous (brown) and endogenous (yellow) FAs by CD8$^+$ T cells stimulated *in vitro* in Glc- or Gal-medium (n=3 samples, pooled from 15 mice/group). (F) Comparison of isotope labeing as $^{13}C_{16}$-palmitate-derived carbon contribution to TCA cycle metabolites in LN cells snap-frozen on dry ice vs. those processed to single cell suspensions and incubated on ice for 2.5 hr (duration of sample processing time for our isotope tracing assays with samples collected from same mice). Data show mean values of % of 1 or 2 ^{13}C-carbon contribution (m+1 or m+2), or total ^{13}C-incorporation rates (total Inc.) into citrate, malate or glutamate (n=3 samples/group, each sample is pooled from LNs of 3-4 mice). (G) MFI and representative histogram of FA uptake by vaccine-induced CD8$^+$ T cells in day 14 or 30 Spl and tumors. (H) MFI and histograms of Cpt1a expression in the same cell subsets as in G. (I) Histograms for CD62L on CD44$^+$CD8$^+$ T cells from day 14 or 30 Spl or tumors. (G-I) n=5/group, representative of 2 assays. (J) Relative intensity of free FAs in the interstitial fluid of day 30 human melanoma PDX tumors over those in sera or interstitial fluids from heart and kidney of same mice (n = 3 for heart, 2 for kidney, 5 for sera and 4 for tumors). (A-E, G-H, J) Data show mean - SEM.

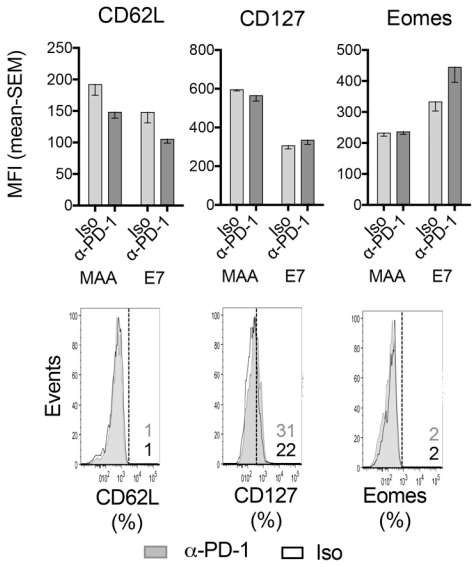

Figure S6, related to Figure 6. **Effects of PD-1 blockade on T cell phenotype**. Top: MFI of markers on/in specific $CD8^+$ TILs from day 30 tumors (n=5-7 mice/group). Below: Representative flow plots for MAA-specific TILs; Iso (open), α-PD-1 (grey).

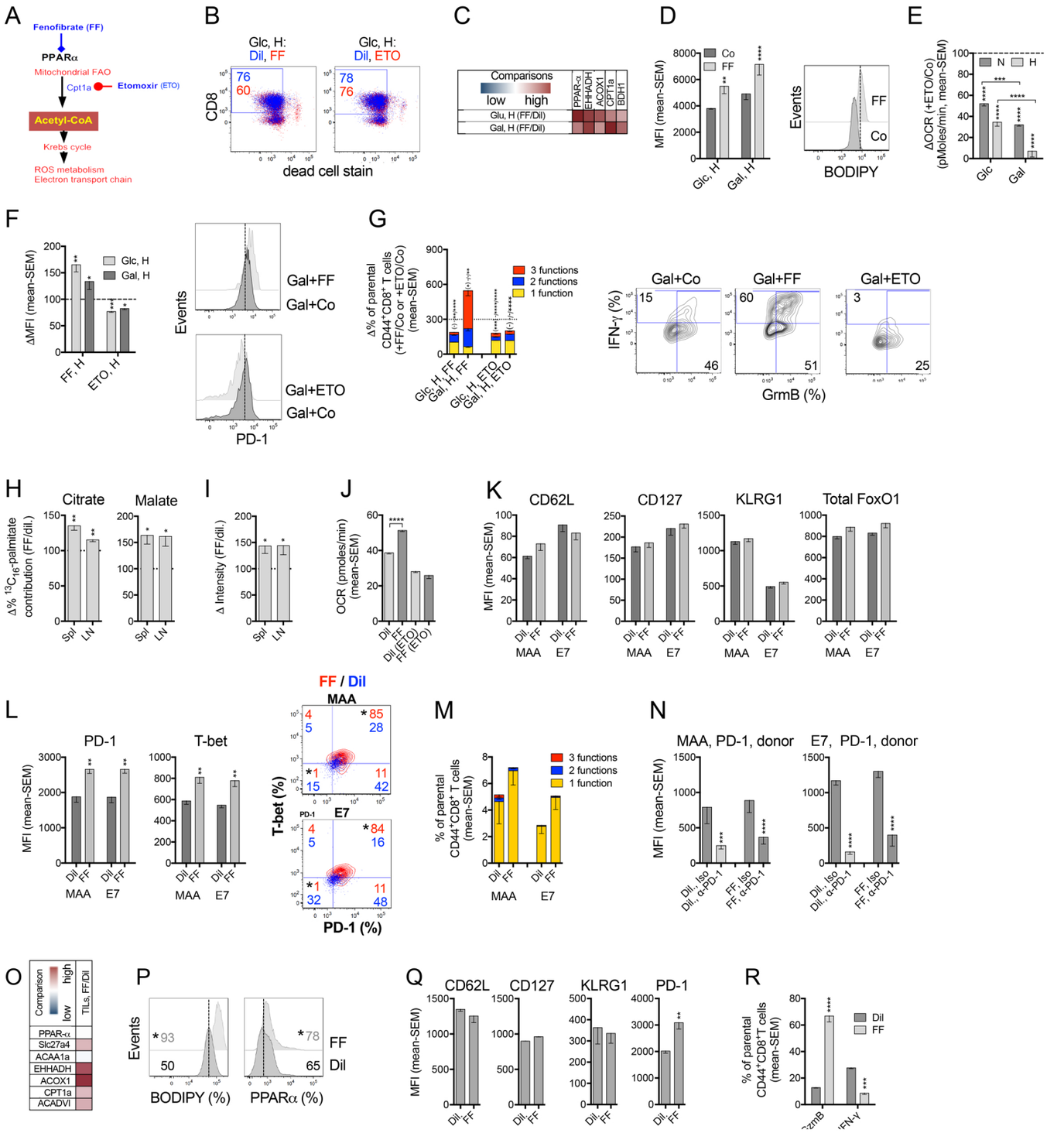

Figure S7, related to Figure 7. Effects of metabolic manipulations of T cells. (A) Cartoon illustrates the working mechanisms of FF or ETO on FA catabolism. Red lines: inhibition; blue: agonist activity. (B) Representative flow plots compare the viabilities of cells cultured in Glc medium under H, and treated with FF or ETO (red) vs. respective diluents (blue). Numbers in plots reflect % live $CD8^+$ T cells over all lymphoblasts within the shown samples. Average % live $CD8^+$ T cells over all lymphoblasts cultured under hypoxia: FF effect: Dil. + Glc: 78 %, FF + Glc: 80 %, Dil. + Gal: 66 %, FF + Gal: 63 %. ETO effect: Dil. + Glc: 68 %, ETO + Glc: 69 %, Dil. + Gal: 65 %, ETO + Gal: 67 %. (C) Transcript levels in $CD8^+$ T cells stimulated *in vitro* in Glc- or Gal-medium with short-term H and treated with FF compared to the corresponding samples treated with Dil. (n=3-4/condition, representative of 2 experiments). (D) BODIPY C_{16} uptake by $CD8^+$ T cells stimulated in Glc- or Gal-medium and subjected to short-term H with addition of FF compared to the corresponding samples treated with Dil. Histogram shows representative samples (n=5, representative of 2 experiments). (E) Relative basal OCR of $CD8^+$ T cells cultured with ETO in Glc- or Gal-medium under N or H normalized to the corresponding samples treated with Dil. * above bars- significant differences between ETO - and Dil.-treated cells. Lines with stars above show differences between the connected samples (n=9, representative of 2 experiments). (F) Left: Effects of FF or ETO on PD-1 expression on $CD8^+$ T cells stimulated under different conditions. Data show relative MFI for PD-1 on cells treated with FF or ETO normalized to those treated with Dil. *: Significant differences between cells treated with FF or ETO compared to Dil-treated cells. Right: representative histograms. (E, F) n=4-6/group, representative of at least 3 experiments. (G) Left: normalized % $CD44^+CD8^+$ T cells producing 3, 2 or 1 of the 3 tested functions. Functions of cells treated with FF or ETO are normalized to those treated with Dil (set at 300, stippled line; n=5/group, representative of 3 assays/group). (*): Significant differences of total responses between cells treated with drug or Dil. * outside of (): significant differences in % of 1,2 and 3 functions (bottom to top). Right: representative flow plots. (H-M) Vaccine model. (H,I) Normalized $^{13}C_{16}$-palmitate contribution to TCA cycle metabolites (H) and 3-hydroxybutyrate intensity (I) in lymphocytes comparing FF to Dil treated mice (n=3, pooled from 4 mice/sample). (J) Basal OCR of $CD8^+$ T cells from Spl of the two groups of donor mice, and pre-treated with or without ETO (n=6/group). (K) MFI values of CD62L, CD127, KLRG1 and total FoxO1 for vaccine-induced specific $CD8^+$ T cells from spleens of mice treated with Dil. or FF for 3 weeks, tested immediately before cell transfer. (L) PD-1 and T-bet on/in specific donor $CD8^+$ T cells from mice treated with Dil or FF. Flow plots: T-bet over PD-1 in MAA-specific $CD8^+$ T cells as overlays of FF (red) vs. Dil (blue). (M) Functions of $CD8^+$ T cells from donor Spl as % of cells producing 3, 2 or 1 of the 3 tested functions. (K-M) n=10/group. (N) PD-1 expression on donor-derived $CD8^+$ TILs recovered from recipients treated with Iso or α-PD-1 (Iso: n=6; α-PD-1: n=7). Experiment was repeated twice. (O-R) OT-1 transfer model. (O) Transcripts comparison in activated OT-1 $CD8^+$ T cells treated *in vitro* with FF vs. Dil. (P) FA uptake and PPAR-α expression by activated OT-1 $CD8^+$ T cells before cell transfer. (Q) Effect of FF treatment on differentiation markers expression on activated OT-1 $CD8^+$ T cells before cell transfer. (R) Functions of OT-1 $CD8^+$ T cells before cell transfer. (O-R) n=3/group, data represent two assays. (D-N, Q, R) Data of bar graphs are shown as mean - SEM.

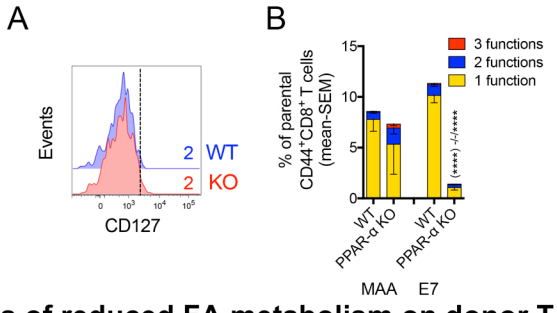

Figure S8, related to Figure 8. Effects of reduced FA metabolism on donor T cells before cell transfer. (A, B) PPARα KO cell transfer model: (A) CD127 histograms for donor MAA-specific $CD8^+$ T cells before transfer. (B) Functions of specific $CD8^+$ T cells from Spl of vaccinated WT and PPAR-α KO mice as % cells producing 3, 2 or 1 of the 3 tested functions before transfer (n=7/group). (A,B) Data represent two assays. (B) Data are shown as mean - SEM.

Table S1, related to the STAR Methods. Primers used for analyzing transcripts levels of enzymes involved in nutrient metabolism of activated $CD8^+$ T cells in vitro and in vivo.

Metabolic pathways	Gene name (Forward-F and Reverse-R)	Primer sequences
Glucose metabolism	mGLUT1-F	TGTGGGAGGAGCAGTGCTCG
	mGLUT1-R	TGGGCTCTCCGTAGCGGTG
	mHK2-F	TGATCGCCTGCTTATTCACGG
	mHK2-R	ACCGCCTAGAAATCTCCAGAAGG
	mPGK1-F	ATGTCGCTTTCCAACAAGCTG
	mPGK1-R	TGGCTCCATTGTCCAAGCAG
	mIDH3a-F	TGGGTGTCCAAGGTCTCTCG
	mIDH3a-R	TCTGGGCCAATTCCATCTCC
	mMDH2-F	TTGGGCAACCCCTTTCACTC
	mMDH2-R	TGTGACTCAGATCTGCTGCCAC
Lipid metabolism regulation, FAs uptake, TG synthesis and lipolysis and FA synthesis	mPPARα-F	AGCCCCATCTGTCCTCTCTCC
	mPPARα-R	TCCAGAGCTCTCCTCACCGATG
	mSLC27A4-F	TGAGTTTGTGGGTCTGTGGCTAGG
	mSLC27A4-R	AAGACAGTGGCGCAGGGCATC

	mSLC27A2-F	TGCTGCTGCTGCCTCTGCTG
	mSLC27A2-R	AGGATGGTACGCACGGGTCG
	mDGAT1-F	ACCTGGCCACAATCATCTGCTTC
	mDGAT1-R	TTGGCCTTGACCCTTCGCTG
	mDGAT2-F	AGCATCCTCTCAGCCCTCCAAG
	mDGAT2-R	TAGCACCAGGAAGGATAGGACC
	mPNPLA2-F	TTCCCGAGGGAGACCAAGTG
	mPNPLA2-R	TGCCGAGGCTCCGTAGATG
	mLIPA-F	TGCTTTCTCGGGTGCCCAC
	mLIPA-R	TCCTCACCAGGATATCCCCAG
Peroxisomal FAO	**mACAA1α-F**	TCCGCTAGGTTCCCGCAGG
	mACAA1α-R	ACAGAAGCTCGTCGGGGGTG
	mEHHADH-F	AAAGTTCGCAAAGGGCAAGG
	mEHHADH-R	TCGCCCAGCTTCACAGAGC
	mACOX1-F	TCCCGATCTGCGCAAGGAG
	mACOX1-R	TGTTCTCCGGACTACCATCCAAG
	mHSD17B4-F	TTGTGAACGACTTAGGAGGGGAC

	mHSD17B4-R	AAATGTGTCCAGTGCCGTCTTC
Mitochondrial FAO	**mACADVL-F**	ACCCTCTCCTCTGATGCTTCCAC
	mACADVL-R	TGAGCACAGATGGGTATGGGAAC
	mACADM-F	AAGCAGGAGCCCGGATTAGG
	mACADM-R	TCCCCGCTTTTGTCATATTCC
Ketone body metabolism	**mBDH1-F**	TCGCCATACTGCATCACCAAG
	mBDH1-R	TGCCAGGTTCCACCACACTG
ROS production/detox-ification and Electron transport chain (ETC)	**mNOX1-F**	AGAAATTCTTGGGACTGCCTTGG
	mNOX1-R	TGCCCCTCAAGAAGGACAGC
	mSOD1-F	ACAGGATTAACTGAAGGCCAGC
	mSOD1-R	TTGCCCAGGTCTCCAACATG
	mCAT-F	TGACATGGTCTGGGACTTCTGG
	mCAT-R	AGCCATTCATGTGCCGGTG
	mCOX5B-F	ACCCGCTCCATGGCTTCTG
	mCOX5B-R	AGTCCCTTCTGTGCTGCTATCATG